Two-Way Teleconnections between the Southern Ocean and the Tropical Pacific via a Dynamic Feedback

YUE DONG, KYLE C. ARMOUR, b.c DAVID S. BATTISTI, DAVID EDWARD BLANCHARD-WRIGGLESWORTH

^a Lamont-Doherty Earth Observatory, Columbia University, Palisades, New York

(Manuscript received 4 February 2022, in final form 2 May 2022)

ABSTRACT: Despite substantial global mean warming, surface cooling has occurred in both the tropical eastern Pacific Ocean and the Southern Ocean over the past 40 years, influencing both regional climates and estimates of Earth's climate sensitivity to rising greenhouse gases. While a tropical influence on the extratropics has been extensively studied in the literature, here we demonstrate that the teleconnection works in the other direction as well, with the southeast Pacific sector of the Southern Ocean exerting a strong influence on the tropical eastern Pacific. Using a slab ocean model, we find that the tropical Pacific sea surface temperature (SST) response to an imposed Southern Ocean surface heat flux forcing is sen-sitive to the longitudinal location of that forcing, suggesting an atmospheric pathway associated with regional dynamics rather than reflecting a zonal-mean energetic constraint. The transient response shows that an imposed Southern Ocean cooling in the southeast Pacific sector first propagates into the tropics by mean-wind advection. Once tropical Pacific SSTs are perturbed, they then drive remote changes to atmospheric circulation in the extratropics that further enhance both Southern Ocean and tropical cooling. These results suggest a mutually interactive two-way teleconnection between the Southern Ocean and tropical Pacific through atmospheric circulations, and highlight potential impacts on the tropics from the extratropical climate changes over the instrumental record and in the future.

KEYWORDS: Pacific Ocean; Southern Ocean; Atmosphere-ocean interaction; Atmospheric circulation; Teleconnections; Climate models; Climate variability; Climate sensitivity

1. Introduction

Observed global sea surface temperatures (SSTs) have exhibited a unique pattern of trends since the early 1980s: despite global mean warming induced by the greenhouse gas forcing, broad cooling has occurred in the tropical eastern Pacific Ocean and the Southern Ocean (Fig. 1). In the tropical Pacific, the enhanced west-east SST zonal gradient has been accompanied with a strengthening of the Walker circulation along with strengthened trade winds (L'Heureux et al. 2013; Kociuba and Power 2015; England et al. 2014). In the Southern Ocean, the observed surface cooling has been accompanied by an expansion of sea ice (Turner et al. 2013; Polvani and Smith 2013; Fan et al. 2014) and surface freshening (Durack and Wijffels 2010; De Lavergne et al. 2014), as well as a positive trend in the southern annular mode (SAM) with intensified and poleward shifted surface westerly winds (Thompson and Solomon 2002; Marshall 2003). The SST trend pattern in the tropical Pacific and the Southern Ocean has had impacts not only on local climates such as tropical precipitation (Ma and Xie 2013; Chadwick et al. 2014) but also on the global warming rate (Kosaka and Xie 2013; Zhou et al. 2016) and on estimates of equilibrium climate sensitivity (ECS) through interactions between SST patterns and radiative feedbacks (Andrews et al. 2018; Ceppi and Gregory 2017; Dong et al. 2019, 2021).

Correctly simulating the observed surface cooling trends in the tropical eastern Pacific and the Southern Ocean remains

Corresponding author: Yue Dong, yd2644@columbia.edu

challenging for global climate models (GCMs; Fyfe et al. 2013; Kociuba and Power 2015; Coats and Karnauskas 2017; Kostov et al. 2018; Luo et al. 2018; Rye et al. 2020; Dong et al. 2021). The fact that GCMs under historical forcings tend to produce warming trends or less-cooling trends over these regions calls into question the fidelity of model projections under greenhouse gas forcing (Plesca et al. 2018; Dong et al. 2021), including the projected long-term warming pattern with enhanced warming in the tropical eastern Pacific and Southern Ocean (Li et al. 2013; Andrews et al. 2015; Dong et al. 2020; Heede et al. 2020). Importantly, this projected longterm warming pattern is expected to give rise to less-negative radiative feedbacks, and therefore higher values of ECS estimates than values inferred from recent observations (Andrews et al. 2018; Marvel et al. 2018; Gregory et al. 2020; Dong et al. 2021).

Yet the causes of the model-observational discrepancy remain unclear. The hypotheses for the observed tropical Pacific SST trend pattern over the last few decades include natural variability in the coupled atmosphere-ocean system inherent to the Pacific basin (Kosaka and Xie 2013; England et al. 2014; Watanabe et al. 2021) and impacts from the Atlantic multidecadal variability through interbasin teleconnection (Wang 2006; Kajtar et al. 2018; Kucharski et al. 2015; McGregor et al. 2014, 2018; Li et al. 2016; Meehl et al. 2021). Others have hypothesized that the observed tropical Pacific SST trend pattern could be a response to external forcings, such as anthropogenic aerosols (Takahashi and Watanabe 2016; Smith et al. 2016; Heede and Fedorov 2021), volcanoes (Gregory et al. 2020), and CO₂ (Seager et al. 2019), with either the forcings

^b Department of Atmospheric Sciences, University of Washington, Seattle, Washington
^c School of Oceanography, University of Washington, Seattle, Washington

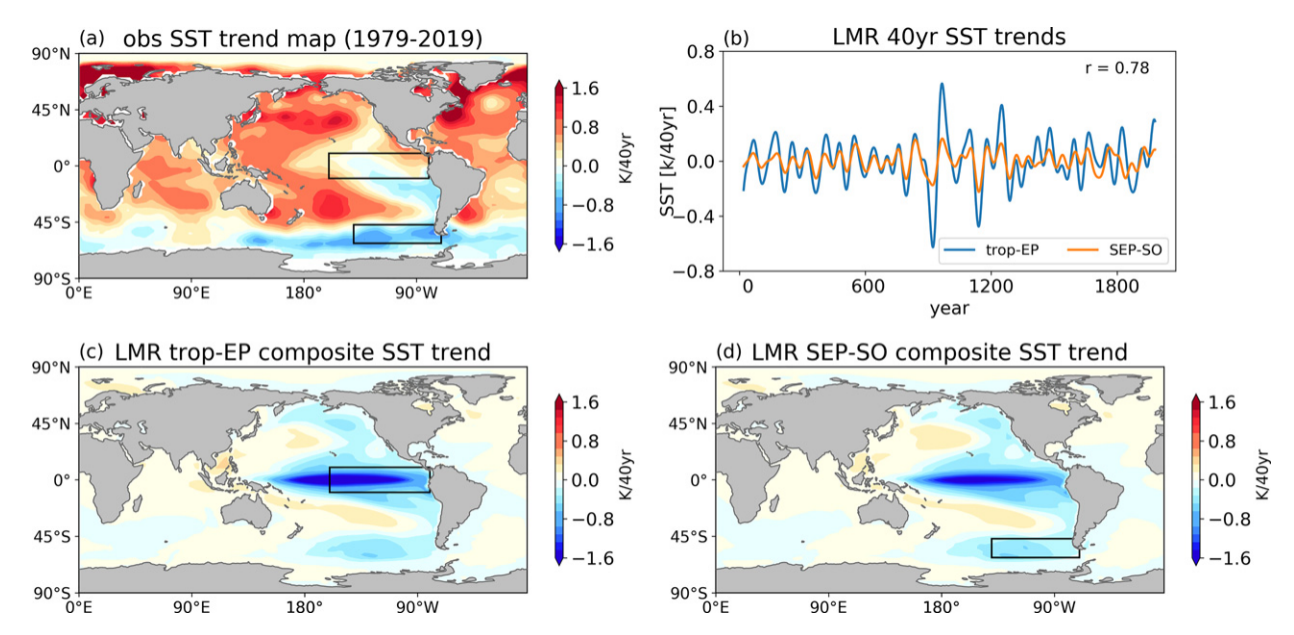


FIG. 1. (a) Observed annual-mean SST trends over 1979–2019 from ERSSTv5b (Huang et al. 2017). (b) Running 40-yr trend of SSTs averaged over the tropical-EP region (108S–108N, 1608–808W) and SEP-SO region (628–478S,1408–708W) from the Last Millennium Reanalysis dataset. Also shown are the composite-mean SST trend patterns associated with significant (c) tropical-EP cooling or (d) SEP-SO cooling. The tropical-EP and SEP-SO regions are illustrated by the black patches in (a), (c), and (d).

or forced responses being misrepresented by models (Kohyama et al. 2017; Coats and Karnauskas 2018; Seager et al. 2019). The observed surface cooling of the Southern Ocean also has multiple potential drivers. While the mean ocean circulation has been proposed to largely account for the delayed Southern Ocean warming in response to greenhouse gas forcing (e.g., Armour et al. 2016), the extent to which the observed surface cooling in the Southern Ocean is caused by external forcing or internal variability remains unclear. It could have resulted from meltwater input from retreating Antarctic ice sheets reducing deep ocean convection (Bintanja et al. 2013; Bronselaer et al. 2018; Purich et al. 2018; Rye et al. 2020), from intensified surface westerlies associated with the positive SAM (Holland and Kwok 2012; Purich et al. 2016; Kostov et al. 2018), or from internal variability (Cabré et al. 2017; Latif et al. 2013; Zhang et al. 2019).

Although there is no consensus on what has caused the observed cooling in the tropical eastern Pacific and the Southern Ocean respectively, the two locations could be connected through teleconnections. The tropical forcing on the extratropics has long been appreciated in the literature through an "atmospheric bridge" via Rossby wave trains generated from changes in tropical convection [e.g., Alexander 1992; Garreaud and Battisti 1999; Ding et al. 2011, 2012; Yuan et al. 2018; see also a recent review by Li et al. (2021)]. The tropical response to extratropical forcing has also been shown in previous studies, with two leading mechanisms proposed to account for different pathways: an atmospheric pathway through zonal-mean energetic constraints and an oceanic pathway through mean ocean circulation. The former has been demonstrated using aquaplanet slab ocean simulations, where tropical precipitation and the Walker circulation have been found to respond to extratropical thermal forcing via anomalous cross-equatorial

atmospheric heat transport, as required by zonal-mean energy budget constraints (Kang et al. 2008, 2009; Hwang and Frierson 2013; Hwang et al. 2017; Kang et al. 2020). The latter has been studied using coupled atmosphere—ocean GCMs, with temperature changes of the tropical upwelled waters traced to temperature changes of the extratropical subducted waters through mean advection by subtropical cells (e.g., Gu and Philander 1997; Burls and Fedorov 2014; Fedorov et al. 2015; Heede et al. 2020).

We find that SSTs over these two key regions (boxes in Fig. 1) closely covary with each other on multidecadal time scales in the past 2000 years in a paleo dataset: the Last Millennium Reanalysis version 2.0 (LMR; Tardif et al. 2019). This paleo reconstruction dataset is derived from the Last Millennium simulations of the Community Climate System Model version 4 (CCSM4), combined with proxy data and linear forward models. In Fig. 1b, we show the running 40-yr trends of 30-yr low-pass filtered annual-mean SSTs, averaged over the tropical eastern Pacific (108S-108N, 1608-808W, denoted herein as "tropical-EP") and part of the Southern Ocean in the southeast Pacific sector that has cooled the most in recent decades (628-478S, 1408-708W, referred to herein as "SEP-SO"). Both regions exhibit low-frequency variabilities that covary with each other (a correlation of 0.78). We then build SST composite maps of tropical-EP warming/cooling trends and SEP-SO warming/cooling trends to look into potential connections between these two regions. Specifically, for tropical-EP composites, we average the global 40-yr trend maps of SSTs over the 40-yr periods where tropical-EP warming or cooling trends exceed two standard deviation. Taking the difference between the warming and cooling compositemean SST trend maps (cooling minus warming) illustrates how

global SSTs are changing when the tropical-EP region is undergoing a substantial cooling on multidecadal time scales (Fig. 1c). The same process is applied for the SEP-SO composite based on SEP-SO 40-yr SST trends (Fig. 1d). The mean SST trend maps of tropical-EP composite and SEP-SO composite show a strong similarity (Figs. 1c,d), with cooling or warming occurring in both regions simultaneously, as expected from the high correlation in Fig. 1b. This common pattern also resembles the pattern of observed SST trends over the past 40 years (Fig. 1a), with cooling in the tropical eastern Pacific and part of the Southern Ocean near the southeast Pacific despite broad warming elsewhere. Note that the LMR dataset exhibits greater decadal-scale SST trends in the tropical eastern Pacific than in the Southern Ocean (Figs. 1b-d), yet the recent observation shows more cooling in the Southern Ocean than in the tropical eastern Pacific. This mismatch may be due to limitations of the LMR reconstruction, which is constrained by both local proxies that are sparse in the Southern Ocean and covariance from the model prior, so the reconstructed Southern Ocean SSTs may lack local information but largely encapsulate remote impacts of the reconstructed tropical SSTs; or it may suggest that something else has influenced Southern Ocean SST trends over the historical record that is not captured by the LMR reconstruction.

These findings suggest that the observed multidecadal cooling trends in the tropical eastern Pacific and the Southern Ocean may be connected and that there may be a two-way teleconnection between these two regions. While the teleconnection from the tropics to the extratropics has been well established, what is less understood is how the Southern Ocean SSTs influence the tropical Pacific SSTs. Thus, the key questions we aim to answer in this study are these: Is the observed tropical eastern Pacific cooling connected to the observed Southern Ocean cooling, particularly in the southeast Pacific sector? If so, what is the mechanism for the two-way teleconnection between these two regions? Furthermore, what implications does this teleconnection have for our interpretation of the recent and future warming patterns? In the following section, we first describe our idealized simulations using a slab ocean model to study the Southern Ocean-tropics teleconnections. In section 3, we propose a new mechanism for the two-way teleconnection between the Southern Ocean and the tropical Pacific, with a dynamic feedback through atmospheric circulation. In section 4, we show that our proposed atmospheric pathway operates within coupled atmosphereocean GCMs. In section 5, we summarize our findings and discuss their potential caveats and implications.

- Idealized Southern Ocean thermal forcing experiments within a slab ocean model
- a. Model setup and experiment design

We first investigate the pathways linking tropical Pacific SST changes and Southern Ocean SST changes using a slab ocean (mixed layer) model with prescribed ocean heat flux convergence ("qflux"). We use a slab ocean version of the Community Atmospheric Model version 4 (CAM4), with a

uniform and annual-mean mixed layer depth of 50 m and horizontal resolution of 1.98 latitude 3 2.58 longitude. There are no interactive ocean dynamics in the slab ocean model, which allows us to separate atmospheric teleconnection pathways from oceanic pathways. In section 4, we further examine the atmospheric pathways in two coupled GCM simulations that include ocean dynamics, finding a strong consistency with our slab ocean results.

We perform a control run and then two qflux-perturbation experiments with anomalous qflux imposed in the tropical-EP or SEP-SO regions}the two regions where SSTs may be mutually connected based on recent observations and the LMR dataset. In both the control run and the experiments, all radiative forcing agents are fixed at year 2000 levels. For the control run, we use an annual-mean qflux climatology constructed from a preindustrial control run within the parent fully coupled model CCSM4. This fully coupled control run has been nudged to reproduce the observed tropical SST climatology (taken from the NOAA ERSSTv3b; Smith et al. 2008) averaged over 1970-2009. The nudging is achieved through adding an annual cycle of additional surface heat fluxes known as the "flux correction" technique (Zhang et al. 2018; Hu and Fedorov 2018). This adjustment largely reduces the common biases in the climatological mean seasonal cycle in fully coupled atmosphere-ocean models, such as a too-cold bias of cold tongue SSTs (Capotondi et al. 2020), too-excessive precipitation off the equator [known as the double intertropical convergence zone (ITCZ) problem; Li and Xie 2014], and the bias in the cross-equatorial winds (Hu and Fedorov 2018). Deriving qflux climatology from the flux-corrected fully coupled control run thus provides a realistic tropical mean state of SST, precipitation, and surface winds in the slab ocean model (Fig. 2a). We only apply this observation-corrected qflux to open waters; for regions where sea ice exists, we use a qflux climatology calculated from a freely evolving preindustrial control run of the fully coupled CCSM4, while keeping the global-mean qflux climatology to be zero (no net gain or loss of heat).

For the qflux-perturbation experiments, we add a constant qflux anomaly of 220 W m²² (i.e., a heat flux divergence from the mixed layer) on top of the qflux control climatology over the tropical-EP or SEP-SO patch. Since the qflux forcing we impose acts as a constant heat sink to the mixed layer, the global mean SSTs are expected to cool toward a new equilibrium until anomalous top-of-atmosphere radiation balances net mixed-layer heat loss. Note that we impose the qflux forcing in localized regions rather than in zonal bands as in previous studies (Kang et al. 2008; Hwang et al. 2017; Stuecker et al. 2020; Kang et al. 2020), which allows us to investigate mechanisms associated with regional dynamics in a more realistic configuration. We run these simulations for 60 years and use an average over the last 30 years to compute the equilibrium responses calculated as the difference between control and qflux-perturbation experiments.

Teleconnections between the tropical-EP and SEP-SO regions in slab ocean simulations

As expected, the imposed qflux forcing drives global mean cooling in both experiments. Despite having smaller global-mean

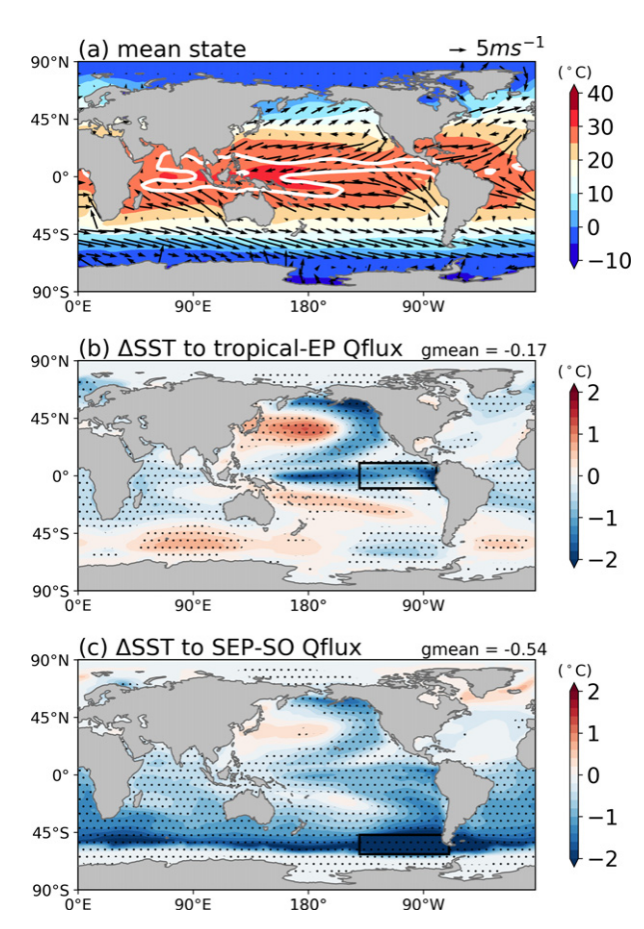


FIG. 2. (a) Mean-state climate of the slab ocean control run. Shading denotes SSTs; arrows denote surface winds; white contour denotes 6 mm day²¹ mean precipitation. (b),(c) SST response to the qflux anomaly imposed in the tropical eastern Pacific (tropical-EP) or the southeast Pacific sector of the Southern Ocean (SEP-SO), respectively. Stippling indicates statistically significant response at the 95% level. The location of the qflux forcing is illustrated by the black patch. The number in the top right in each panel denotes the global mean of the SST response.

qflux anomalies, the extratropical qflux forcing produces greater global-mean cooling than the tropical aflux forcing (Fig. 2b). This is consistent with the result of earlier studies (Rose et al. 2014; Kang and Xie 2014) that the high-latitude surface heat flux forcing is more efficient at changing global temperatures than the tropical forcing, revealed by multiple slab ocean models with distinct zonal-mean qflux forcings. The spatial patterns of SST changes in these two experiments also exhibit some common features. The qflux forcing in the tropical-EP patch drives remote SST changes extending to the extratropics, yielding SST cooling in the vicinity of the SEP-SO patch in the southeast Pacific sector of the Southern Ocean (Fig. 2b). The affux forcing in the SEP-SO patch in turn drives substantial tropical cooling, with more cooling in the eastern Pacific than in the western Pacific, producing a La Niña-like tropical SST pattern (Fig. 2c). These simulations are consistent with the results of the LMR dataset}the tropical eastern Pacific and the Southern Ocean

near the southeastern Pacific can influence each other, resulting in same-sign SST changes in both regions. Moreover, the results from the slab ocean model suggest that the teleconnection between these regions can be established through atmospheric pathways without ocean circulations.

The prevailing atmospheric pathway proposed for the extratropics-to-tropics teleconnection has been linked to a zonal-mean energetic constraint, derived from idealized simulations with zonal-mean extratropical thermal forcing (Kang et al. 2008, 2009; Hwang et al. 2017; Kang et al. 2020). That is, an anomalous interhemispheric gradient in an imposed forcing is expected to induce anomalous cross-equatorial atmospheric heat transport, accomplished via Hadley cell adjustment. As a result, the ITCZ tends to shift toward the warmer hemisphere (i.e., away from the hemisphere with a negative qflux forcing), resulting in changes in the surface winds and zonal SST contrast through wind–evaporation–SST (WES) feedback (Xie and Philander 1994).

To test this theory, we next show three similar slab ocean experiments, with the same zonal-mean qflux forcing imposed over the same latitudes (558–358S) but over different longitude bands. Here we add a uniform qflux anomaly of 215 W m²² (heat flux divergence from the mixed layer) in the southwest Pacific (1308E–1708W), southeast Pacific (1408–808W), and South Atlantic (608W–08), illustrated in Figs. 3a–c respectively. These patches are located slightly north of the SEP-SO patch shown previously, to avoid potential impacts of changes to the sea ice edge. All three patch simulations are run for 60 years, following the same setup described in the previous section.

In all cases, the imposed qflux forcing drives broad surface cooling and an increase in precipitation in the northern branch of the ITCZ, consistent with previous studies (Hwang et al. 2017; Kang et al. 2020). The zonal-mean precipitation changes (Fig. 3g) and zonal-mean SST changes (Fig. 3h) are similar across cases, suggesting that the zonal-mean climate changes are indeed largely determined by the zonal-mean forcing. However, the degree of zonal asymmetry of tropical SST changes varies by case (Fig. 3i). When the qflux forcing is imposed in the southeast Pacific, a strong and significant cooling occurs in the tropical eastern Pacific, forming a La Niña-like tropical SST pattern (Fig. 3b). This anomalous zonal SST gradient is weaker in the other two runs (Figs. 3a,c; also see Fig. 3i), which suggests that the Southern Ocean-to-tropics teleconnection is not solely dependent on the zonal mean energetics and instead depends on the region over which that forcing is applied. Interestingly, the strongest teleconnection to the tropical Pacific is from the southeast Pacific, which is also the region in the Southern Ocean that is most influenced by the tropical qflux forcing (Fig. 2b) and where observations have showed the greatest cooling trends since approximately the 1980s (Fig. 1a). A key question follows: Why does this region produce a particularly strong Southern Ocean-tropical Pacific teleconnection?

3. Mechanisms for the Southern Ocean-to-tropical Pacific atmospheric teleconnection

To investigate the mechanism for the teleconnection from the southeast Pacific to the tropical Pacific, we first look into

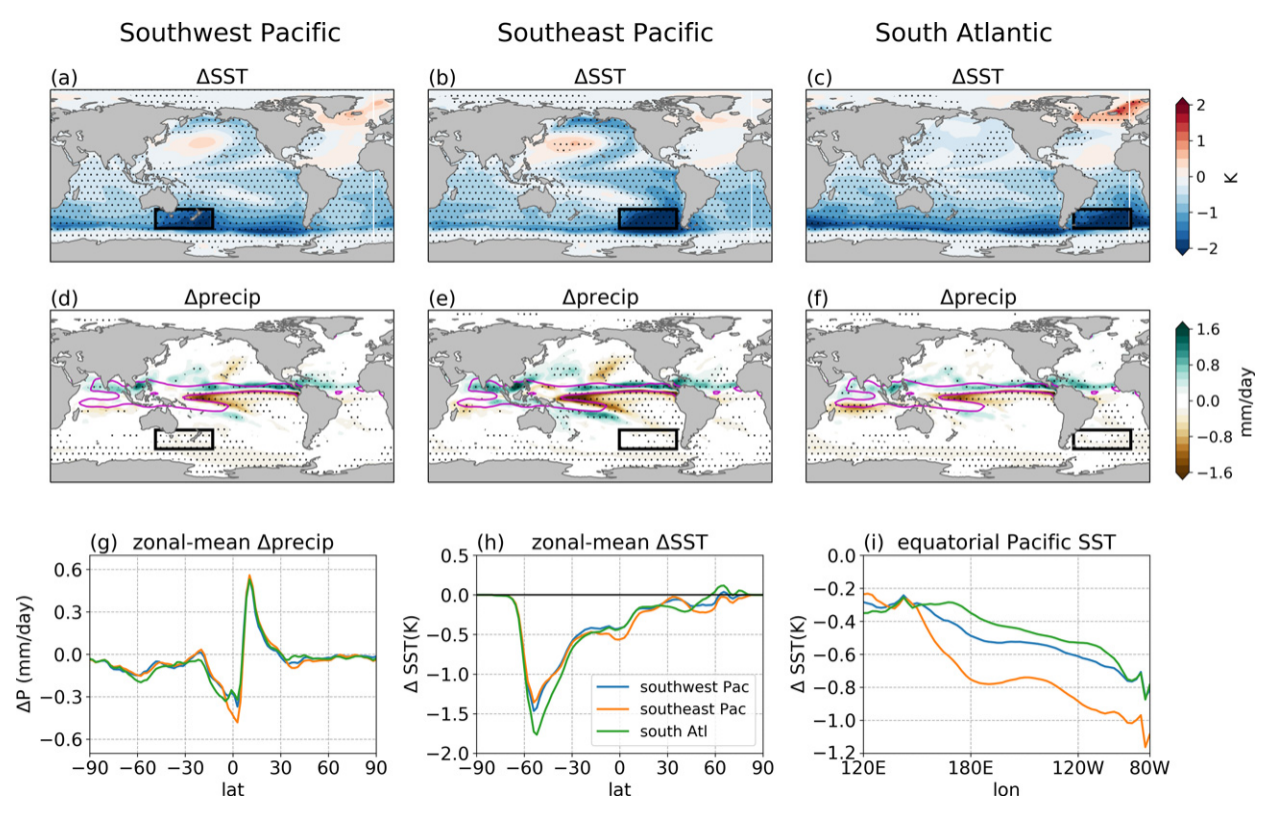


Fig. 3. Responses to qflux anomaly imposed in the (left) southwest Pacific, (center) southeast Pacific, and (right) South Atlantic. (a)–(c) Changes in SST. (d)–(f) Changes in precipitation. Pink lines denote the mean-state precipitation of 6 mm day²¹ from control run (same as the white contour in Fig. 2a). (g) Zonal mean changes of precipitation. (h) Zonal mean changes of SST. (i) Changes of SST in the equatorial Pacific averaged over 58S–58N. Stippling in (a)–(f) indicates statistically significant response at the 95% level.

the time evolution of transient response in the slab ocean run forced by the southeast Pacific qflux anomaly shown in the above section (Fig. 3b), demonstrating two stages of the teleconnection with a positive feedback associated with atmospheric circulation changes (section 3a). We then validate the dynamical process of the positive feedback by additional prescribed-SST simulations within an atmospheric GCM (AGCM; section 3b). Finally, we show that changes in atmospheric circulation needed for the teleconnection have occurred in observations (section 3c).

a. Slab ocean transient response reveals a dynamic positive feedback

To examine the transient response in the slab ocean run, we perform an ensemble of 20 members with the same qflux forcing in the southeast Pacific as in Fig. 3b (i.e., a uniform qflux anomaly of 215 W m²² added over 558–358S, 1408–808W). Each is branched from a different day of January in the control simulation and run for 6 years. We present results from the average of the 20 ensemble members to reduce noise from random natural variability, and below we only show the ensemble mean responses that are statistically different from zero at 95% level.

Figure 4 shows that over the first 2 years, the Southern Ocean SSTs over the patch of qflux forcing cool substantially, with relatively little cooling outside the patch. But by year 3, a weak cooling signal reaches the southeast tropical Pacific,

enhancing the climatological east-west SST gradient (Fig. 4c, left column). The weak cooling in the southeastern tropical Pacific is not accompanied by a robust change in the surface winds over the tropics on this time scale. This suggests that the leading process for the extratropical to tropical teleconnection at this first stage is advection by climatological mean winds. The mean-state surface westerlies over the Southern Ocean forcing patch blow toward the Andes in high latitudes, and deflect equatorward and merge to form the southeasterly trade winds in the southeast tropical Pacific (Fig. 2a), resulting in a climatological subtropical high sea level pressure (SLP). Hence, the climatological mean winds can efficiently advect surface temperature anomalies from the southeast Pacific to the tropical eastern Pacific. However, the advection by the mean winds only results in a weak cooling in the tropical eastern Pacific during this first stage (by year 3).

The first stage is followed by a more substantial cooling of the tropical Pacific in year 4, accompanied by anomalously strong trade winds in the Pacific (Fig. 4d, left column). While the trade winds in general can be influenced by multiple processes, we find that the strengthening of the trade winds in year 4 is primarily caused by a strengthening of subtropical high SLP in both hemispheres (Fig. 4d, middle column), which itself is a result of tropics-originated Rossby wave teleconnections. As shown in Fig. 4, the weak cooling in the tropical eastern

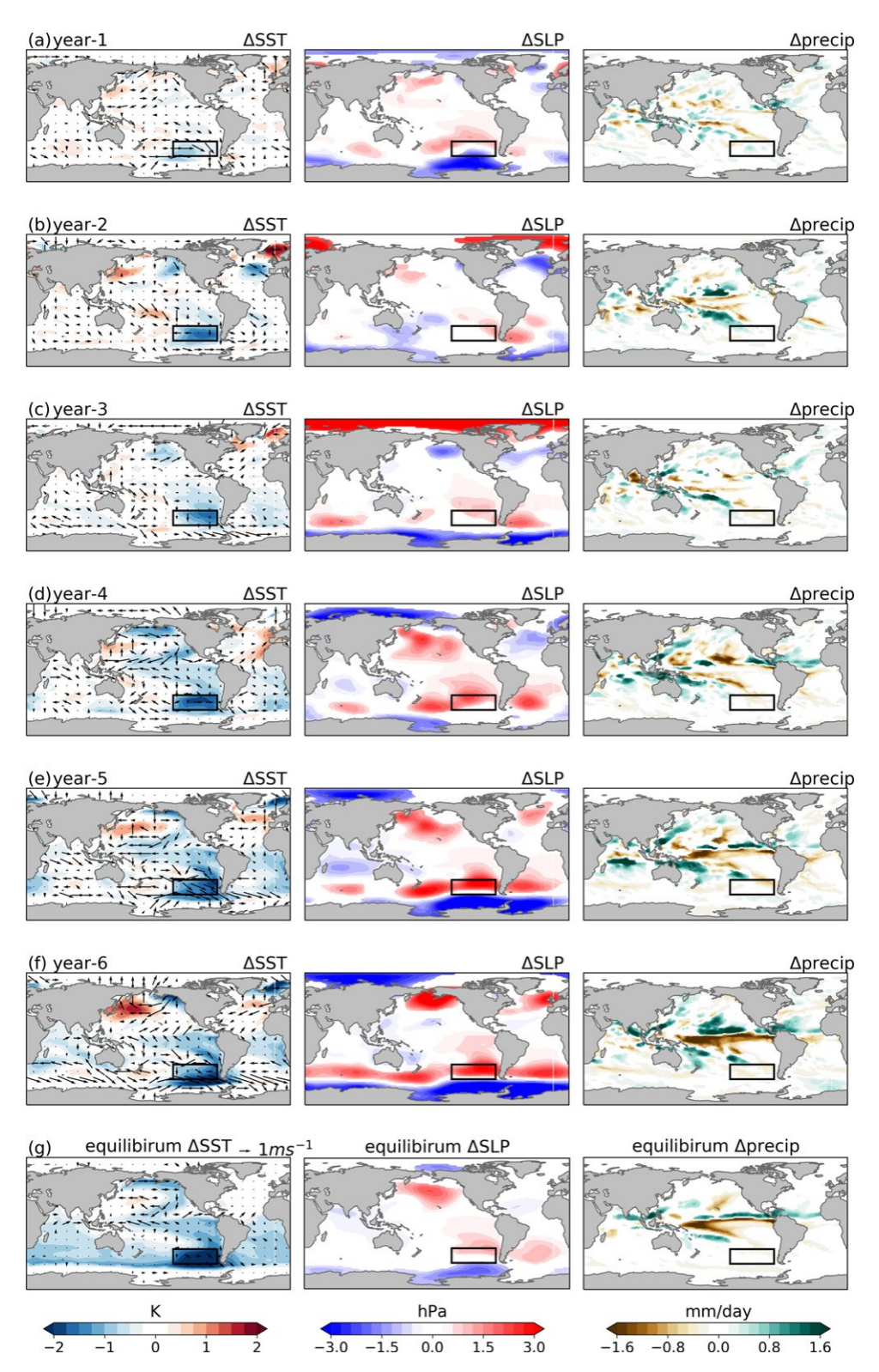


Fig. 4. (a)–(f) Annual mean changes of (left) SST (shading) and surface winds (arrows), (center) SLP, and (right) net precipitation in the first 6 years averaged over the 20 members of southeast Pacific qflux ensemble. The imposed qflux forcing is as same as in the equilibrium run shown in Fig. 3b. (g) The equilibrium responses (from the equilibrium run shown in Fig. 3, averaged over years 31–60). For all panels, only statistically significant ensemble-mean responses above the 95% level are shown.

Pacific that is developed in the first stage (by year 3) forms a La Niña-like tropical SST pattern (Fig. 4c, left column), causing atmospheric convection to contract westward over the Maritime Continent (Figs. 4c, right column). The increase in convective heating in the far western Pacific and a decrease in the central Pacific forces anomalous Rossby wave teleconnections toward higher latitudes, yielding anomalous strengthening of the subtropical highs in the southeast Pacific and the North Pacific in year 4 (Fig. 4d, middle column; see also Garreaud and Battisti 1999). The subtropical SLP anomalies amplify the trade winds in the tropics in both hemispheres, which cause further cooling in the tropical eastern Pacific via the WES feedback. Additionally, in the Southern Hemisphere (SH) extratropics, the subtropical SLP anomalies enhance southerly flows in the southeast Pacific and westerlies in the vicinity of the cooling patch in the Southern Ocean (Fig. 4d, left column). The anomalous southerly flows lead to further tropical cooling via anomalous advection from the Southern Ocean toward the tropics. The anomalous extratropical westerlies cause further cooling near the Southern Ocean forcing patch via increased evaporation, which can be ultimately advected into the tropics by both climatological mean winds and the strengthened southeasterlies associated with SLP anomalies. Together, these tropically induced circulation changes can feed back onto the tropical SSTs by amplifying the tropical eastern Pacific cooling}a positive feedback of the mutually interactive teleconnection between the Southern Ocean and the tropical Pacific.

In summary, the response to an imposed southeast Pacific qflux forcing evolves in two stages. First, over years 1-3, a small portion of the qflux-forced Southern Ocean cooling in the southeast Pacific propagates to the tropical southeast Pacific by way of advection by climatological mean winds. Since this stage mostly involves atmosphere-ocean thermal coupling, its time scale depends on the time scale of the mixed-layer adjustment, which is on the order of 2 years in our simulations that used a uniform 50-m mixed layer. Second, once the tropical eastern Pacific cooling emerges, changes in the location of the tropical convective heating produce Rossby wave teleconnections to the extratropics, enhancing the trade winds, SH extratropical winds, and Southern Ocean cooling}all of which are conducive to further amplifying the cooling in the southeast tropical Pacific (though by decomposing the total anomalous advection, we find changes in tropical and extratropical winds contribute more than changes in Southern Ocean surface temperatures). This positive feedback between the extratropics and the tropics in stage 2 appears to account for the majority of the equilibrium tropical SST response to the imposed Southern Ocean cooling (cf. Figs. 4d and 4g). Although persisting to equilibrium, this stage develops quickly once the tropical Pacific zonal SST gradient begins to change (from year 3 to year 4) because it is mostly mediated by changes in atmospheric circulation. The two stages of the teleconnection and their time scales can also be seen in the transient zonal-mean SST response averaged globally (Fig. 5), with a slow propagation of cooling from the Southern Ocean to the tropics in years 2-3, followed by an enhancement of cooling in both the tropics and the Southern Ocean in year 4, which persists to the end of the integration.

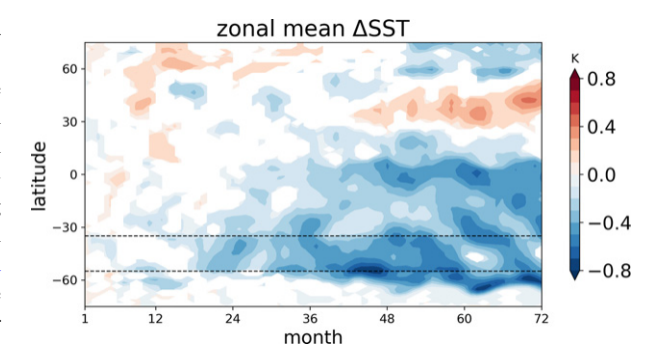


FIG. 5. Monthly zonal-mean SST response to the southeast Pacific qflux forcing over the first 6 years. Only statistically significant ensemble-mean responses above the 95% level are shown. The dashed lines illustrate the latitudes of the imposed qflux forcing (558–358S), although the qflux forcing is applied not over the entire zonal band but only in the southeast Pacific sector (1408–808W).

Prescribed-SST simulations confirm the tropical origin of the positive feedback

The slab ocean transient response reveals a positive feedback in the second stage associated with changes in extratropical atmospheric circulation. While the tropical origin of the subtropical SLP changes seen in year 4 has long been appreciated in the literature through Rossby wave dynamics (e.g., Alexander 1992; Garreaud and Battisti 1999; Ding et al. 2011, 2012), in this subsection we perform additional experiments to confirm that the extratropical atmospheric circulation changes in the second stage arise due to the tropical SST change rather than the qflux-forced Southern Ocean SST change.

We use the same atmospheric model (CAM4) as was used in the coupled slab ocean model, except in an AGCM setup where SSTs and sea ice concentration are prescribed everywhere. Consistent with the slab ocean simulations, the prescribed-SST simulations also use a modern-day observed SST climatology, and all radiative forcing agents are fixed at year 2000 levels. On top of those SSTs, we prescribe the annual-mean equilibrium SST anomalies induced by the southeast Pacific qflux forcing (applied in the slab ocean ensemble in section 3a) onto different regions separately. Both the control simulation and SST-perturbed simulations are run for 15 years; the responses are averaged over the last 10 years.

In the first simulation, we prescribe SST anomalies only within the southeast Pacific qflux forcing patch (i.e., the same patch illustrated in Fig. 4), while keeping SSTs over the rest of global oceans unchanged (Fig. 6a), to test if the SH subtropical SLP anomalies could be driven by the qflux-forced Southern Ocean cooling. We find that this extratropical SST forcing only drives weak and local SLP changes, without much remote influence on the subtropical SLP or tropical surface winds (Fig. 6d). In the second simulation, we instead prescribe SST anomalies within the tropical Pacific (208S–208N, 1208E–808W), with most of the cooling in the eastern Pacific (Fig. 6b). This tropical SST forcing drives substantial responses at global scale that extend to the high latitudes in both hemispheres. Notably, it produces a pattern of SLP and surface

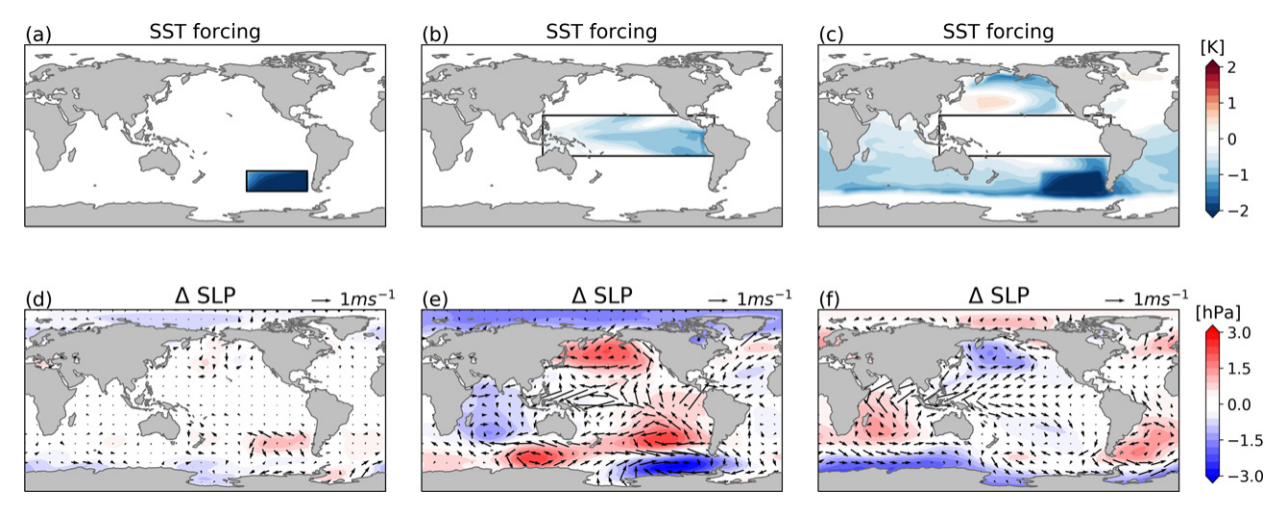


Fig. 6. Prescribed SST simulations and their responses. (a)–(c) Prescribed SST anomalies in the southeast Pacific (the same patch shown in Fig. 4), the tropical Pacific, and global oceans except the tropical Pacific, respectively. (d)–(f) SLP and surface winds responses to the corresponding SST forcing. All the SST anomalies are taken from the annual-mean equilibrium SST changes in the southeast Pacific qflux experiment (left panel of Fig. 4g). The tropical Pacific is defined as 1208E–808W, 208S–208N.

winds that resembles the pattern of transient climate response starting in year 4 in Fig. 4, featuring a heightening of subtropical highs in both hemispheres, as well as strengthened southeasterly trade winds in the tropical Pacific and strengthened surface westerlies in the southeast Pacific sector of the Southern Ocean. To further illustrate the comparison between tropical Pacific SST forcing and extratropical SST forcing, we perform another simulation where we prescribe the SST anomalies induced by the southeast Pacific qflux forcing throughout the global ocean except over the tropical Pacific (Fig. 6c). This broad extratropical SST forcing (which includes some tropical regions in the Indian Ocean and the Atlantic Ocean) has little impact on the SH subtropical SLP in the Pacific sector, and even produces an opposite sign of the Northern Hemisphere subtropical SLP and tropical surface winds (Fig. 6f).

Thus, these prescribed-SST simulations confirm that the changes in the subtropical SLP and associated surface winds that arise in year 4 (the second stage) are not directly forced by the cooling in the Southern Ocean, but are instead due to a teleconnection forced by SST changes in the tropical Pacific, which were born from the SST changes in the Southern Ocean through advection by mean winds.

c. The two-way teleconnection between the Southern Ocean and the tropics in observations

Based on both the slab ocean and the AGCM prescribed-SST simulations, we find that there is a two-way teleconnection between the Southern Ocean and tropical Pacific. SST changes in the southeast Pacific sector of the Southern Ocean can trigger teleconnections to the tropical eastern Pacific through advection by mean winds. In turn, tropical Pacific SST changes can drive remote changes to extratropical atmospheric circulation that are conducive to amplifying SST changes in both the tropical eastern Pacific and the southeast Pacific sector of the Southern Ocean. This finding suggests that the observed multi-decadal surface cooling in the Southern Ocean and tropical

eastern Pacific may be mutually connected and amplified by

Indeed, the key circulation changes needed for the teleconnection can also be seen in observations and the LMR dataset. In Fig. 7a, we show the 40-yr trends of annual-mean SLP and 10-m surface winds over 1979-2019 from ERA5 reanalysis data (Hersbach et al. 2020). The observed trend pattern highlights a strengthening of the subtropical highs in the Pacific in both hemispheres, along with strengthened trade winds in the tropical eastern Pacific and strengthened westerlies in the southeast Pacific sector of the Southern Ocean. In addition, we repeat the composite analysis with the LMR dataset (as done for Figs. 1c and 1b), except computing 40-yr trend maps of global SLP associated with substantial cooling of the tropical-EP and SEP-SO regions. The composite-mean SLP trend maps also show similar features with a strengthening of the subtropical highs in both hemispheres (Figs. 7b,c). Both datasets show a pattern of circulation changes consistent with the results of our simulations.

However, these findings are not sufficient to determine whether the observed teleconnection is activated by a tropical change or a Southern Ocean change in the first place, or whether the initial surface cooling (over either of these two regions) is driven by internal variability or external forcing. While the underlying causes of the observed SST trend patterns remain to be further investigated, in the following section we discuss one possible perspective that the observed eastern tropical Pacific cooling trends may be driven by recent changes in the Southern Ocean.

Tropical Pacific SST response to Southern Ocean non-thermal forcings in fully coupled simulations

Having established a mechanism for the two-way atmospheric teleconnection between the tropical Pacific and the Southern Ocean, next we evaluate whether the mechanism

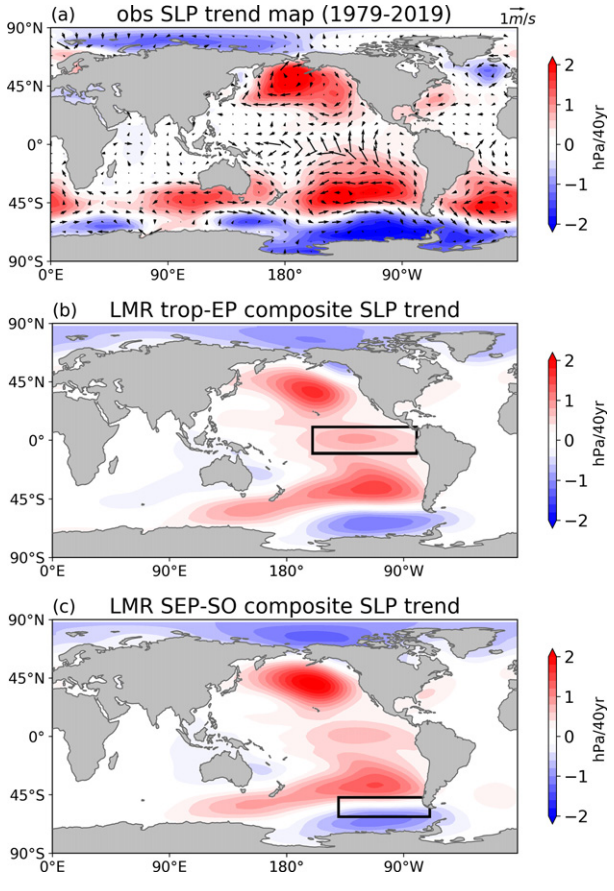


FIG. 7. (a) Observed annual-mean SLP (shading) and 10-m surface winds (arrows) trends over 1979–2019 from ERA5. (b),(c) Composite mean of 40-yr SLP trends, associated with significant cooling trends in the EP and SO regions respectively (consistent with Figs. 1c,d).

operates in coupled atmosphere-ocean GCM simulations from two recently published studies that applied non-thermal forcings over the Southern Ocean: one simulates the effects of Antarctic meltwater discharge to the Southern Ocean (Sadai et al. 2020) and the other simulates the effects of changes in SH extratropical atmospheric circulation (Blanchard-Wrigglesworth et al. 2021). By analyzing the results of tropical SST responses in these studies, we address two questions: Does the atmospheric teleconnection found in our slab ocean results also exist in a fully coupled configuration with dynamic oceans? What implications does this teleconnection have for observed and projected warming patterns?

a. The impacts of Southern Ocean meltwater input

First, we show a set of meltwater "hosing" experiments using the fully coupled Community Earth System Model version 1 with the Community Atmosphere Model version 5 (CESM1-CAM5), provided by Sadai et al. (2020). These simulations account for meltwater input from Antarctic ice sheet melting over the twenty-first century}a process that is not represented in CMIP5 and CMIP6 GCMs. Here we present results from two simulations of Sadai et al. (2020): a control

run and a hosing run, both of which are driven by identical radiative forcing (using representative concentration pathway RCP8.5) over 2005–2100. The control run includes increasing freshwater input driven only by increasing precipitation over Antarctica that is discharged into the Southern Ocean, reaching $\mathbb{B}0.2$ Sv (1 Sv $\equiv 10^6$ m³ s²¹) by the end of the twenty-first century. The hosing run takes into account additional timevariant and spatially distributed meltwater and iceberg discharge from Antarctic ice sheets into the Southern Ocean [see details in Sadai et al. (2020)]. The total amount of the added meltwater input in the hosing run reaches $\mathbb{B}1$ Sv by the end of the twenty-first century, estimated by an offline ice sheet model forced by the same RCP8.5 scenario (see Fig. 1B in Sadai et al. 2020).

Figure 8 shows the SST and SLP trend maps over the twenty-first century from the control run and the hosing run of Sadai et al. (2020). While the RCP8.5 forcing results in a considerable amount of warming nearly all over the globe in the control run (Fig. 8a), the imposed meltwater input in the hosing run cools the Southern Ocean SSTs, increases the extent of Antarctic sea ice, and reduces the rise of global mean surface temperatures (Fig. 8c; see also Sadai et al. 2020), consistent with the results of other meltwater forcing studies using different models (e.g., Bronselaer et al. 2018; Purich et al. 2018; Rye et al. 2020). The Antarctic-meltwater induced Southern Ocean surface cooling in this hosing run is further transported to the tropics, mostly manifested in the eastern Pacific, forming a La Niña-like warming pattern (Fig. 8e). Accompanying the surface temperature cooling is a strengthened SH subtropical high in the southeast Pacific (Fig. 8f), which acts to enhance the tropical surface cooling as discussed earlier. While the teleconnection from the Southern Ocean to the tropical Pacific seen here on a centennial time scale could also be in part driven by oceanic responses, such as enhanced ocean heat transport by mean subtropical cells (Gu and Philander 1997; Fedorov et al. 2015) or by strengthened subtropical cells (Luo et al. 2017; Heede et al. 2020), this fully coupled simulation shows all the same features seen in our slab ocean results, consistent with our proposed atmospheric pathway.

Although the results of Sadai et al. (2020) may depend on the model used and the amount of meltwater applied (which is likely to be at the high end of future projections), it has important implications for understanding recent and future global surface warming patterns. A growing body of literature has suggested that Antarctic meltwater forcing may be partially responsible for the observed surface cooling and sea ice expansion over the Southern Ocean (e.g., Bronselaer et al. 2018; Bintanja et al. 2013; Rye et al. 2020), although the results published so far appear to be highly model dependent. Antarctic meltwater induced Southern Ocean surface cooling could be further transported to the tropics via advection by mean winds, considering the results of Sadai et al. (2020), driving tropical eastern Pacific cooling through the two-way teleconnections described here. This hypothesis provides a plausible explanation for the cause of the observed cooling trends in both the tropical eastern Pacific and Southern Ocean seen in the past four decades.

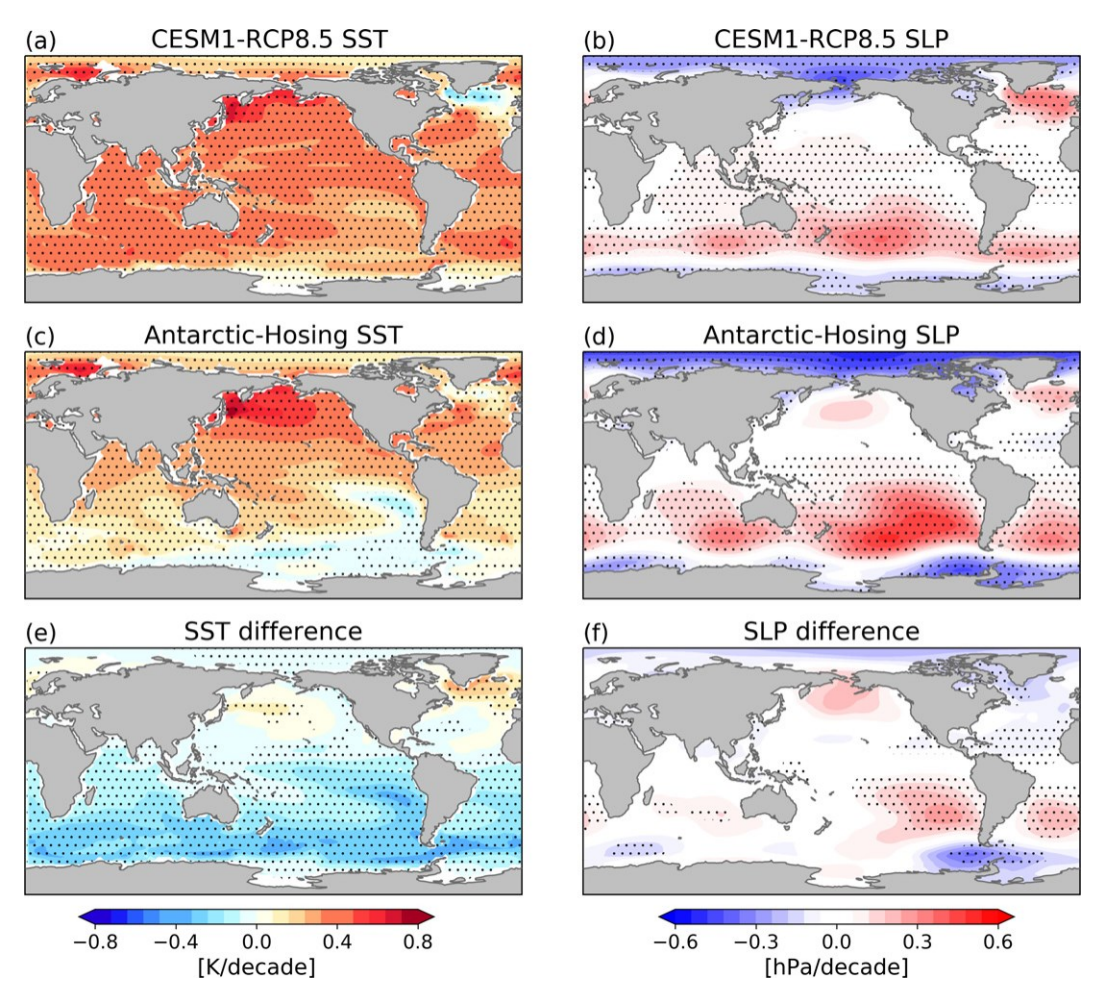


Fig. 8. (left) SST and (right) SLP linear trends over 2005–2100 from the (a) CESM1 control run and (b) CESM1 Antarctic meltwater hosing run, as in Sadai et al. (2020). Both simulations are under RCP8.5 forcing scenario. (e),(f) The difference between the control run and the hosing run that reflects the response to the imposed meltwater forcing. Stippling indicates statistically significant linear trends at the 95% level. Data courtesy of Shaina Sadai.

b. The impacts of Southern Ocean winds

Next, we show an ensemble of Southern Ocean wind-nudging experiments over 1979-2018 (Fig. 9), extending the simulations published in Blanchard-Wrigglesworth et al. (2021). These experiments are also performed using the fully coupled CESM1-CAM5. All simulations are run under historical radiative forcing from 1979 to 2005 and RCP 8.5 forcing from 2006 to 2018, consistent with the CESM1 Large Ensemble simulations (LENS; Kay et al. 2015). We present results averaged from five ensemble members; each member is initiated from a different LENS member from January 1980. The novelty of these wind-nudging experiments is that, throughout the full period, zonal and meridional winds poleward of 458S in the SH are nudged to 6-hourly ERA-Interim reanalysis data (Dee et al. 2011) from 850 hPa to the top of the model. Note that in Blanchard-Wrigglesworth et al. (2021) the nudging is applied poleward of 458 in both hemispheres, while here we show results from five newly performed runs that are otherwise identical but apply the wind nudging over 458–908S in the SH only.

By construction, these simulations are forced to reproduce the observed strengthening of the westerly winds over the Southern Ocean, which is generally underestimated and located farther south in LENS (see Fig. 3 in Blanchard-Wrigglesworth et al. 2021). Furthermore, because the model has to maintain thermal wind balance by increasing SLP gradient in the SH extratropics in response to the intensified polar winds, these wind-nudging experiments also produce positive SLP trend anomalies near the SH subtropical high than in the LENS, largely resembling the observed SLP trend pattern (Fig. 9d). With an anomalously deep SH subtropical high, these wind-nudging experiments produce cooling trends in the tropical eastern Pacific, which are not seen in the LENS ensemble mean, despite the fact that no Southern Ocean SST forcing was directly applied. Although the wind forcing induces some cooling in the Southern Ocean (Fig. 9e), this local cooling is not significant and is much weaker than that observed. Therefore, even without strong Southern Ocean cooling to initiate the teleconnection, extratropical circulation changes can cause a significant tropical eastern

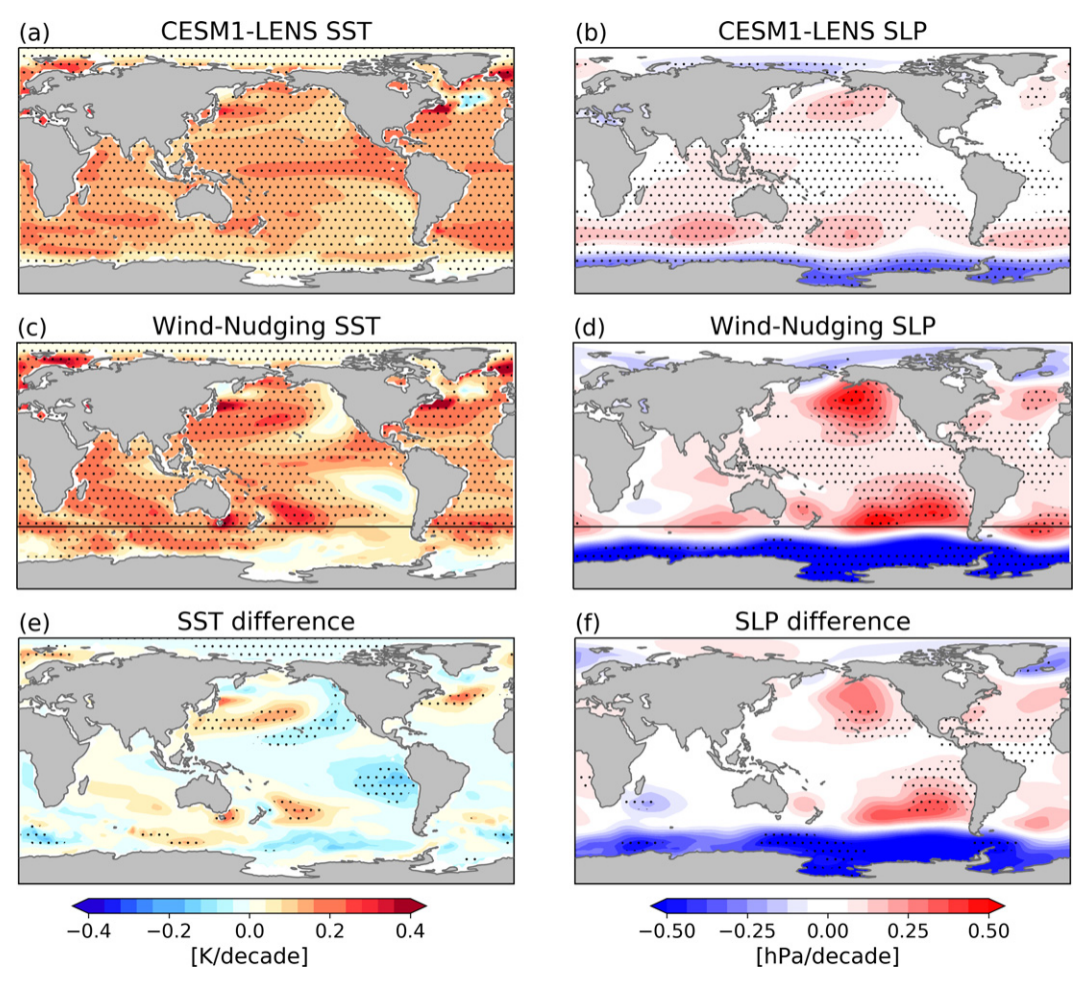


Fig. 9. (left) SST and (right) SLP linear trends over 1979–2018 from (a),(b) CESM1 LENS ensemble mean and (c),(d) CESM1 wind-nudging experiments (average of 5 ensemble members, where atmospheric winds are nudged to reanalysis only south of 458S), and (e),(f) the difference between the wind-nudging experiments and LENS, which reflects the response to the imposed Southern Ocean winds. Stippling indicates statistically significant linear trends at the 95% level.

Pacific cooling response (Fig. 9e). These simulations thus illustrate the second stage of the teleconnection we found in our slab ocean results whereby the SLP anomalies in the subtropics enhance the southeasterly trade winds, which cause cooling in tropical southeast Pacific. Indeed, in the tropical southeast Pacific, overlying the anomalous surface cooling is the strengthened surface winds in these wind-nudging experiments, which are not found in the LENS ensemble mean.

Even though these wind-nudging experiments only capture the second stage of the mechanism we proposed, the fact that the teleconnection can be established without initial Southern Ocean SST forcing highlights a dominant role of atmospheric circulation changes in linking the Southern Ocean to the tropical Pacific. Moreover, the results of these fully coupled simulations suggest that atmospheric forcing is sufficient to drive the Southern Ocean-to-tropics teleconnection, although it remains unclear to what extent and how oceanic circulation changes contribute to the atmospheric teleconnection.

5. Summary and discussion

Using a set of slab ocean simulations and AGCM fixed-SST simulations, we found that there is a two-way teleconnection between the Southern Ocean and tropical Pacific. An imposed Southern Ocean cooling can first propagate into the tropics through advection by climatological mean winds over the southeast Pacific. Once the tropical Pacific SSTs are perturbed, this tropical SST forcing can drive remote changes to extratropical atmospheric circulation through Rossby wave teleconnections, featuring anomalously deep subtropical highs in both hemispheres, which results in strengthened trade winds in the tropics and strengthened surface westerlies in the Southern Ocean. These wind anomalies are conducive to further enhancing the surface cooling in both the tropical eastern Pacific and the southeast Pacific of the Southern Ocean. That is, the tropics-forced circulation changes exert a positive feedback on the two-way teleconnection process. These circulation changes along with the SST changes in the tropical Pacific and the Southern Ocean have also been observed over the past 40 years.

Although we did not evaluate potential oceanic pathways, we showed tropical Pacific SST responses to changes in the Southern Ocean in two sets of fully coupled simulations that are consistent with our proposed atmospheric teleconnection pathway. One is the meltwater hosing experiments provided by Sadai et al. (2020), where Southern Ocean SSTs are changed owing to the addition of meltwater input from Antarctic ice sheets. The other is the wind-nudging experiment extended from the simulations published in Blanchard-Wrigglesworth et al. (2021), where the extratropical circulation is changed through nudging Antarctic winds to observations. Neither of these simulations imposed a direct thermal forcing in the Southern Ocean, but both showed a La Niña-like tropical SST response to the imposed changes over the Southern Ocean. The results of these two studies provide further evidence for our proposed atmospheric pathway in a fully coupled configuration linking the tropical Pacific response to Southern Ocean forcings. That said, on longer time scales, it is expected that oceanic response may also contribute to the connection between the Southern Ocean and the tropical Pacific, through anomalous advection by mean subtropical cells with anomalous extratropical surface temperatures or by changes in the subtropical cells. Indeed, early studies (Kay et al. 2016; Kang et al. 2020) have found that in some models the oceanic responses tend to dampen the atmospheric teleconnection. Therefore, the impacts of dynamic oceans on the atmospheric teleconnections need to be further quantified.

One implication of this study is that the observed tropical eastern Pacific cooling trends over recent decades could, at least in part, be driven by changes in the SH extratropics. One potential driver is the observed Southern Ocean surface cooling, which may have been induced by Antarctic meltwater input and may continue in the form of muted Southern Ocean warming over the twenty-first century (Sadai et al. 2020). Another potential driver is changes in the SH extratropical circulation featuring strengthened surface westerlies over the Southern Ocean (Blanchard-Wrigglesworth et al. 2021), which may have arisen from both atmospheric internal variability and anthropogenic forcing (e.g., stratospheric ozone depletion). In either case, SH extratropical climate change can influence the tropics through teleconnections, driving tropical eastern Pacific cooling which, in turn, can impact global climate through interactions with climate feedbacks (Zhou et al. 2016; Dong et al. 2019, 2021). This hypothesis provides a new perspective on the current understanding of the observed tropical Pacific SST trend pattern, accounting for the impacts from the SH extratropics through teleconnections. The results suggest a need to revisit the projected long-term warming pattern with enhanced warming in both the Southern Ocean and tropical eastern Pacific from current GCMs, which have no representation of increased meltwater from Antarctica.

These findings come with caveats. First, the results we presented may be sensitive to the model and forcing used in this study. The slab ocean simulations and fully coupled simulations used in this study are all based on variations of CESM, and therefore the results and conclusions could be model dependent. In

addition, in our slab ocean simulations, we used an arbitrary qflux forcing (uniform 215 W m²² at each grid box). A stronger idealized thermal forcing in the SH extratropics is also found to be effective in driving the tropical Pacific SST response within other various slab ocean models (Kang et al. 2020). However, we note a recent "pacemaker" study by Zhang et al. (2021), where the Southern Ocean SSTs are nudged to time-varying observed SST anomalies over 1979-2013, yet the ensemble mean of these simulations produced little change in the tropical Pacific SST trends. Several reasons could account for these disparate results. First, although the Southern Ocean SSTs in the pacemaker simulations are nudged toward the observed evolution of SST anomalies, this SST forcing may be too small in their model to generate significant teleconnection responses. Note that in our slab ocean simulations we find that only a small portion of the directly imposed Southern Ocean cooling can transport to the tropics by mean-wind advection. It is also possible that a potential atmospheric teleconnection from this small Southern Ocean SST change could be to some extent damped by dynamic oceans in the fully coupled model of Zhang et al. (2021). Additionally, the absence of the teleconnection to the tropics in the pacemaker simulations may be partly due to model biases in the mean state (e.g., a double ITCZ bias may lead to biases in the SH crossequatorial winds), which are largely corrected in our slab ocean runs. Thus, our proposed Southern Ocean-to-tropics atmospheric teleconnection need to be further quantified in a range of models.

Another caveat of our results is that the Southern Oceanto-tropics teleconnection may depend on the radiative effect of tropical low clouds. Several recent studies have found that low clouds over the tropical eastern Pacific stratocumulus deck play a primary role in the zonal-mean heat transport and therefore extratropics-to-tropics teleconnection (e.g., Hwang et al. 2017; Kang et al. 2020; Chen et al. 2021; Shin et al. 2021). Surface cooling over the tropical eastern Pacific of the descending region will increase local lower tropospheric stability measured by the estimated inversion strength (EIS), which allows for more low clouds to occur (Wood and Bretherton 2006). Because low clouds have a strong surface cooling effect through reflecting incoming solar radiation back to space, the growing of low clouds will then strengthen the shortwave reflection and therefore further cool the surface}a positive feedback associated with cloud radiative effect (CRE). Indeed, in our Southern Ocean qflux simulations, we also see increases in low cloud cover and enhanced reflection of shortwave radiative fluxes at the top of atmosphere in all three runs over the tropical eastern Pacific along with surface cooling (not shown). While the impacts of CRE warrant further quantification, we argue that this SST-cloud coupling is initially activated by changes in the tropical Pacific SSTs, which themselves are driven by Southern Ocean cooling via mean-wind advection. As shown in Fig. 3, the qflux forcing in the southwest Pacific and South Atlantic produces weaker tropical eastern Pacific cooling (Figs. 3a,c) and less increase in low clouds (not shown) than the qflux forcing in the southeast Pacific (Fig. 3b), even though the cloud physics is unchanged in the model. This is owing to a less efficient "trigger" (i.e., the advection by mean winds near the southeast Pacific) in these two simulations.

Thus, although the CRE of low clouds could amplify the tropical eastern Pacific cooling, the initial advection from the Southern Ocean by mean winds is essential to the tropical SST changes.

Understanding how the observed SST trend pattern has developed and how it will evolve in the future is crucial to achieving accurate climate change projections. In this study, we have investigated the possibility that the observed tropical eastern Pacific cooling is connected to the observed Southern Ocean cooling most prominent in the southeast Pacific sector through an atmospheric pathway. This mechanism provides a new perspective to our understanding of the tropical response to extratropical forcing, accounting for the regional dynamics and atmospheric circulation. It also raises a possibility that model deficiencies in reproducing the observed tropical Pacific SST trend pattern may be traced to model deficiencies in accurately representing changes in the Southern Ocean, such as Antarctic meltwater input or changes in SH extratropical atmospheric circulation. Although our results may be sensitive to the model and forcing applied, if the meltwater input and/or SH extratropical circulation does prove to have as large an impact on tropical climates as our results suggest, there will be a need to revisit GCM projections of past and future global warming patterns.

Acknowledgments. We thank Aaron Levine for providing CCSM4 flux-correction simulations, Shaina Sadai for sharing CESM1 meltwater hosing simulations, and Xiyue Zhang for sharing CESM1 Southern Ocean pacemaker simulations. We thank Cecilia Bitz and Sarah Kang for insightful discussions. YD and KCA were supported by National Science Foundation Grant AGS-1752796 and the National Oceanic and Atmospheric Administration MAPP Program (Award NA20OAR4310391). KCA was supported by an Alfred P. Sloan Research Fellowship (Grant FG-2020-13568). EBW was supported by National Science Foundation Antarctic Program PLR1643436. YD and DSB were supported by the Tamaki Foundation.

Data availability statement. The slab ocean simulations and CAM4 prescribed-SST simulations performed in this study are available at http://hdl.handle.net/1773/48142.

REFERENCES

- Alexander, M. A., 1992: Midlatitude atmosphere–ocean interaction during El Niño. Part I: The North Pacific Ocean. J. Climate, 5, 944–958, https://doi.org/10.1175/1520-0442(1992)005,0944: MAIDEN.2.0.CO:2.
- Andrews, T., J. M. Gregory, and M. J. Webb, 2015: The dependence of radiative forcing and feedback on evolving patterns of surface temperature change in climate models. J. Climate, 28, 1630–1648, https://doi.org/10.1175/JCLI-D-14-00545.1.
- } } , and Coauthors, 2018: Accounting for changing temperature patterns increases historical estimates of climate sensitivity. Geophys. Res. Lett., 45, 8490-8499, https://doi.org/10.1029/ 2018GL078887.

- Armour, K. C., J. Marshall, J. R. Scott, A. Donohoe, and E. R. Newsom, 2016: Southern Ocean warming delayed by circumpolar upwelling and equatorward transport. Nat. Geosci., 9, 549–554, https://doi.org/10.1038/ngeo2731.
- Bintanja, R., G. J. van Oldenborgh, S. S. Drijfhout, B. Wouters, and C. A. Katsman, 2013: Important role for ocean warming and increased ice-shelf melt in Antarctic sea-ice expansion. Nat. Geosci., 6, 376–379, https://doi.org/10.1038/ngeo1767.
- Blanchard-Wrigglesworth, E., L. A. Roach, A. Donohoe, and Q. Ding, 2021: Impact of winds and Southern Ocean SSTs on Antarctic sea ice trends and variability. J. Climate, 34, 949–965, https://doi.org/10.1175/JCLI-D-20-0386.1.
- Bronselaer, B., M. Winton, S. M. Griffies, W. J. Hurlin, K. B. Rodgers, O. V. Sergienko, R. J. Stouffer, and J. L. Russell, 2018: Change in future climate due to Antarctic meltwater. Nature, 564, 53–58, https://doi.org/10.1038/s41586-018-0712-z.
- Burls, N. J., and A. V. Fedorov, 2014: What controls the mean east-west sea surface temperature gradient in the equatorial Pacific: The role of cloud albedo. J. Climate, 27, 2757–2778, https://doi.org/10.1175/JCLI-D-13-00255.1.
- Cabré, A., I. Marinov, and A. Gnanadesikan, 2017: Global atmospheric teleconnections and multidecadal climate oscillations driven by Southern Ocean convection. J. Climate, 30, 8107–8126, https://doi.org/10.1175/JCLI-D-16-0741.1.
- Capotondi, A., C. Deser, A. S. Phillips, Y. Okumura, and S. M. Larson, 2020: ENSO and Pacific decadal variability in the Community Earth System Model version 2. J. Adv. Model. Earth Syst., 12, e2019MS002022, https://doi.org/10.1029/2019MS002022.
- Ceppi, P., and J. M. Gregory, 2017: Relationship of tropospheric stability to climate sensitivity and Earth's observed radiation budget. Proc. Natl. Acad. Sci. USA, 114, 13 126–13 131, https:// doi.org/10.1073/pnas.1714308114.
- Chadwick, R., P. Good, T. Andrews, and G. Martin, 2014: Surface warming patterns drive tropical rainfall pattern responses to CO₂ forcing on all timescales. Geophys. Res. Lett., 41, 610–615, https://doi.org/10.1002/2013GL058504.
- Chen, Y. J., Y. T. Hwang, and P. Ceppi, 2021: The impacts of cloud-radiative changes on poleward atmospheric and oceanic energy transport in a warmer climate. J. Climate, 34, 7857–7874, https://doi.org/10.1175/JCLI-D-20-0949.1.
- Coats, S., and K. B. Karnauskas, 2017: Are simulated and observed twentieth century tropical Pacific sea surface temperature trends significant relative to internal variability? Geophys. Res. Lett., 44, 9928–9937, https://doi.org/10.1002/2017GL074622.
- } } , and } } , 2018: A role for the Equatorial Undercurrent in the ocean dynamical thermostat. J. Climate, 31, 6245–6261, https://doi.org/10.1175/JCLI-D-17-0513.1.
- Dee, D. P., and Coauthors, 2011: The ERA-Interim reanalysis: Configuration and performance of the data assimilation system. Quart. J. Roy. Meteor. Soc., 137, 553–597, https://doi.org/10.1002/qj.828.
- de Lavergne, C., J. B. Palter, E. D. Galbraith, R. Bernardello, and I. Marinov, 2014: Cessation of deep convection in the open Southern Ocean under anthropogenic climate change. Nat. Climate Change, 4, 278–282, https://doi.org/10.1038/nclimate2132.
- Ding, Q., E. J. Steig, D. S. Battisti, and M. Küttel, 2011: Winter warming in West Antarctica caused by central tropical Pacific warming. Nat. Geosci., 4, 398–403, https://doi.org/10.1038/ ngeo1129.
- } } , } } , and J. M. Wallace, 2012: Influence of the tropics on the southern annular mode. J. Climate, 25, 6330–6348, https://doi.org/10.1175/JCLI-D-11-00523.1.

- Dong, Y., C. Proistosescu, K. C. Armour, and D. S. Battisti, 2019: Attributing historical and future evolution of radiative feed-backs to regional warming patterns using a Green's function approach: The preeminence of the western Pacific. J. Climate, 32, 5471–5491, https://doi.org/10.1175/JCLI-D-18-0843.1.
- } } , K. C. Armour, M. D. Zelinka, C. Proistosescu, D. S. Battisti, C. Zhou, and T. Andrews, 2020: Intermodel spread in the pattern effect and its contribution to climate sensitivity in CMIP5 and CMIP6 models. J. Climate, 33, 7755–7775, https:// doi.org/10.1175/JCLI-D-19-1011.1.
- } } , and Coauthors, 2021: Biased estimates of equilibrium climate sensitivity and transient climate response derived from historical CMIP6 simulations. Geophys. Res. Lett., e2021GL095778, https://doi.org/10.1029/2021GL095778.
- Durack, P. J., and S. E. Wijffels, 2010: Fifty-year trends in global ocean salinities and their relationship to broad-scale warming. J. Climate, 23, 4342–4362, https://doi.org/10.1175/2010JCLI3377.1.
- England, M. H., and Coauthors, 2014: Recent intensification of wind-driven circulation in the Pacific and the ongoing warming hiatus. Nat. Climate Change, 4, 222–227, https://doi.org/10. 1038/nclimate2106.
- Fan, T., C. Deser, and D. P. Schneider, 2014: Recent Antarctic sea ice trends in the context of Southern Ocean surface climate variations since 1950. Geophys. Res. Lett., 41, 2419–2426, https://doi.org/10.1002/2014GL059239.
- Fedorov, A. V., N. J. Burls, K. T. Lawrence, and L. C. Peterson, 2015: Tightly linked zonal and meridional sea surface temperature gradients over the past five million years. Nat. Geosci., 8, 975–980, https://doi.org/10.1038/ngeo2577.
- Fyfe, J. C., N. P. Gillett, and F. W. Zwiers, 2013: Overestimated global warming over the past 20 years. Nat. Climate Change, 3, 767–769, https://doi.org/10.1038/nclimate1972.
- Garreaud, R., and D. S. Battisti, 1999: Interannual (ENSO) and interdecadal (ENSO-like) variability in the Southern Hemisphere tropospheric circulation. J. Climate, 12, 2113–2123, https://doi.org/10.1175/1520-0442(1999)012,2113:IEAIEL.2. 0.CO:2.
- Gregory, J. M., T. Andrews, P. Ceppi, T. Mauritsen, and M. J. Webb, 2020: How accurately can the climate sensitivity to CO₂ be estimated from historical climate change? Climate Dyn., 54, 129–157, https://doi.org/10.1007/s00382-019-04991-y.
- Gu, D., and S. G. Philander, 1997: Interdecadal climate fluctuations that depend on exchanges between the tropics and extratropics. Science, 275, 805–807, https://doi.org/10.1126/science.275.5301.805.
- Heede, U. K., and A. V. Fedorov, 2021: Eastern equatorial Pacific warming delayed by aerosols and thermostat response to CO₂ increase. Nat. Climate Change, 11, 696–703, https://doi. org/10.1038/s41558-021-01101-x.
- } } , and N. J. Burls, 2020: Time scales and mechanisms for the tropical Pacific response to global warming: A tug of war between the ocean thermostat and weaker Walker. J. Climate, 33, 6101–6118, https://doi.org/10.1175/JCLI-D-19-0690.1.
- Hersbach, H., and Coauthors, 2020: The ERA5 global reanalysis. Quart. J. Roy. Meteor. Soc., 146, 1999–2049, https://doi.org/10. 1002/qj.3803.
- Holland, P. R., and R. Kwok, 2012: Wind-driven trends in Antarctic sea-ice drift. Nat. Geosci., 5, 872–875, https://doi.org/10.1038/ ngeo1627.
- Hu, S., and A. V. Fedorov, 2018: Cross-equatorial winds control El Nino diversity and change. Nat. Climate Change, 8, 798–802, https://doi.org/10.1038/s41558-018-0248-0.

- Huang, B., and Coauthors, 2017: Extended Reconstructed Sea Surface Temperature, version 5 (ERSSTv5): Upgrades, validations, and intercomparisons. J. Climate, 30, 8179–8205, https://doi.org/10.1175/JCLI-D-16-0836.1.
- Hwang, Y. T., and D. M. Frierson, 2013: Link between the double-Intertropical Convergence Zone problem and cloud biases over the Southern Ocean. Proc. Natl. Acad. Sci. USA, 110, 4935–4940, https://doi.org/10.1073/pnas.1213302110.
- } } , S.-P. Xie, C. Deser, and S. M. Kang, 2017: Connecting tropical climate change with Southern Ocean heat uptake. Geophys. Res. Lett., 44, 9449–9457, https://doi.org/10.1002/ 2017GL074972.
- Kajtar, J. B., A. Santoso, S. McGregor, M. H. England, and Z. Baillie, 2018: Model under-representation of decadal Pacific trade wind trends and its link to tropical Atlantic bias. Climate Dyn., 50, 1471–1484, https://doi.org/10.1007/s00382-017-3699-5.
- Kang, S. M., and S.-P. Xie, 2014: Dependence of climate response on meridional structure of external thermal forcing. J. Climate, 27, 5593–5600, https://doi.org/10.1175/JCLI-D-13-00622.1.
- } } , I. M. Held, D. M. Frierson, and M. Zhao, 2008: The response of the ITCZ to extratropical thermal forcing: Idealized slab-ocean experiments with a GCM. J. Climate, 21, 3521–3532, https://doi.org/10.1175/2007JCLI2146.1.
- } } , D. M. Frierson, and I. M. Held, 2009: The tropical response to extratropical thermal forcing in an idealized GCM: The importance of radiative feedbacks and convective parameterization. J. Atmos. Sci., 66, 2812–2827, https://doi.org/10.1175/ 2009JAS2924.1.
- } } , S.-P. Xie, Y. Shin, H. Kim, Y.-T. Hwang, M. F. Stuecker, B. Xiang, and M. Hawcroft, 2020: Walker circulation response to extratropical radiative forcing. Sci. Adv., 6, eabd3021, https://doi.org/10.1126/sciadv.abd3021.
- Kay, J. E., and Coauthors, 2015: The Community Earth System Model (CESM) large ensemble project: A community resource for studying climate change in the presence of internal climate variability. Bull. Amer. Meteor. Soc., 96, 1333–1349, https://doi.org/10.1175/BAMS-D-13-00255.1.
- } } , C. Wall, V. Yettella, B. Medeiros, C. Hannay, P. Caldwell, and C. Bitz, 2016: Global climate impacts of fixing the Southern Ocean shortwave radiation bias in the Community Earth System Model (CESM). J. Climate, 29, 4617–4636, https://doi.org/10. 1175/JCLI-D-15-0358.1.
- Kociuba, G., and S. B. Power, 2015: Inability of CMIP5 models to simulate recent strengthening of the Walker circulation: Implications for projections. J. Climate, 28, 20–35, https:// doi.org/10.1175/JCLI-D-13-00752.1.
- Kohyama, T., D. L. Hartmann, and D. S. Battisti, 2017: La Ninalike mean-state response to global warming and potential oceanic roles. J. Climate, 30, 4207–4225, https://doi.org/10. 1175/JCLI-D-16-0441.1.
- Kosaka, Y., and S. P. Xie, 2013: Recent global-warming hiatus tied to equatorial Pacific surface cooling. Nature, 501, 403–407, https://doi.org/10.1038/nature12534.
- Kostov, Y., D. Ferreira, K. C. Armour, and J. Marshall, 2018: Contributions of greenhouse gas forcing and the southern annular mode to historical Southern Ocean surface temperature trends. Geophys. Res. Lett., 45, 1086–1097, https://doi.org/10. 1002/2017GL074964.
- Kucharski, F., F. S. Syed, A. Burhan, I. Farah, and A. Gohar, 2015: Tropical Atlantic influence on Pacific variability and mean state in the twentieth century in observations and

- CMIP5. Climate Dyn., 44, 881–896, https://doi.org/10.1007/s00382-014-2228-z.
- Latif, M., T. Martin, and W. Park, 2013: Southern Ocean sector centennial climate variability and recent decadal trends. J. Climate, 26, 7767–7782, https://doi.org/10.1175/JCLI-D-12-00281.1.
- L'Heureux, M. L., S. Lee, and B. Lyon, 2013: Recent multidecadal strengthening of the Walker circulation across the tropical Pacific. Nat. Climate Change, 3, 571–576, https://doi.org/ 10.1038/nclimate1840.
- Li, C., J. S. von Storch, and J. Marotzke, 2013: Deep-ocean heat uptake and equilibrium climate response. Climate Dyn., 40, 1071–1086, https://doi.org/10.1007/s00382-012-1350-z.
- Li, G., and S.-P. Xie, 2014: Tropical biases in CMIP5 multimodel ensemble: The excessive equatorial Pacific cold tongue and double ITCZ problems. J. Climate, 27, 1765–1780, https://doi. org/10.1175/JCLI-D-13-00337.1.
- Li, X., S.-P. Xie, S. T. Gille, and C. Yoo, 2016: Atlantic-induced pantropical climate change over the past three decades. Nat. Climate Change, 6, 275–279, https://doi.org/10.1038/nclimate2840.
- } } , and Coauthors, 2021: Tropical teleconnection impacts on Antarctic climate changes. Nat. Rev. Earth Environ., 2, 680–698, https://doi.org/10.1038/s43017-021-00204-5.
- Luo, J. J., G. Wang, and D. Dommenget, 2018: May common model biases reduce CMIP5's ability to simulate the recent Pacific La Niña-like cooling? Climate Dyn., 50, 1335–1351, https://doi.org/10.1007/s00382-017-3688-8.
- Luo, Y., J. Lu, F. Liu, and O. Garuba, 2017: The role of ocean dynamical thermostat in delaying the El Niño-like response over the equatorial Pacific to climate warming. J. Climate, 30, 2811–2827, https://doi.org/10.1175/JCLI-D-16-0454.1.
- Ma, J., and S.-P. Xie, 2013: Regional patterns of sea surface temperature change: A source of uncertainty in future projections of precipitation and atmospheric circulation. J. Climate, 26, 2482–2501, https://doi.org/10.1175/JCLI-D-12-00283.1.
- Marshall, G. J., 2003: Trends in the southern annular mode from observations and reanalyses. J. Climate, 16, 4134–4143, https:// doi.org/10.1175/1520-0442(2003)016,4134:TITSAM.2.0.CO;2.
- Marvel, K., R. Pincus, G. A. Schmidt, and R. L. Miller, 2018: Internal variability and disequilibrium confound estimates of climate sensitivity from observations. Geophys. Res. Lett., 45, 1595–1601, https://doi.org/10.1002/2017GL076468.
- McGregor, S., A. Timmermann, M. F. Stuecker, M. H. England, M. Merrifield, F. F. Jin, and Y. Chikamoto, 2014: Recent Walker circulation strengthening and Pacific cooling amplified by Atlantic warming. Nat. Climate Change, 4, 888–892, https://doi.org/10.1038/nclimate2330.
- } } , M. F. Stuecker, J. B. Kajtar, M. H. England, and M. Collins, 2018: Model tropical Atlantic biases underpin diminished Pacific decadal variability. Nat. Climate Change, 8, 493–498, https://doi.org/10.1038/s41558-018-0163-4.
- Meehl, G. A., and Coauthors, 2021: Atlantic and Pacific tropics connected by mutually interactive decadal-timescale processes. Nat. Geosci., 14, 36–42, https://doi.org/10.1038/s41561-020-00669-x.
- Plesca, E., V. Grützun, and S. A. Buehler, 2018: How robust is the weakening of the Pacific Walker circulation in CMIP5 idealized transient climate simulations? J. Climate, 31, 81–97, https://doi.org/10.1175/JCLI-D-17-0151.1.
- Polvani, L. M., and K. L. Smith, 2013: Can natural variability explain observed Antarctic sea ice trends? New modeling evidence from CMIP5. Geophys. Res. Lett., 40, 3195–3199, https://doi.org/10.1002/grl.50578.

- Purich, A., W. Cai, M. H. England, and T. Cowan, 2016: Evidence for link between modelled trends in Antarctic sea ice and underestimated westerly wind changes. Nat. Commun., 7, 10409, https://doi.org/10.1038/ncomms10409.
- } , M. H. England, W. Cai, A. Sullivan, and P. J. Durack, 2018: Impacts of broad-scale surface freshening of the Southern Ocean in a coupled climate model. J. Climate, 31, 2613–2632, https://doi.org/10.1175/JCLI-D-17-0092.1.
- Rose, B. E., K. C. Armour, D. S. Battisti, N. Feldl, and D. D. Koll, 2014: The dependence of transient climate sensitivity and radiative feedbacks on the spatial pattern of ocean heat uptake. Geophys. Res. Lett., 41, 1071–1078, https://doi.org/10.1002/2013GL058955.
- Rye, C. D., J. Marshall, M. Kelley, G. Russell, L. S. Nazarenko, Y. Kostov, G. A. Schmidt, and J. Hansen, 2020: Antarctic glacial melt as a driver of recent Southern Ocean climate trends. Geophys. Res. Lett., 47, e2019GL086892, https://doi.org/10.1029/2019GL086892.
- Sadai, S., A. Condron, R. DeConto, and D. Pollard, 2020: Future climate response to Antarctic ice sheet melt caused by anthropogenic warming. Sci. Adv., 6, eaaz1169, https://doi.org/ 10.1126/sciadv.aaz1169.
- Seager, R., M. Cane, N. Henderson, D. E. Lee, R. Abernathey, and H. Zhang, 2019: Strengthening tropical Pacific zonal sea surface temperature gradient consistent with rising greenhouse gases. Nat. Climate Change, 9, 517–522, https://doi.org/ 10.1038/s41558-019-0505-x.
- Shin, Y., S. M. Kang, K. Takahashi, M. F. Stuecker, Y. T. Hwang, and D. Kim, 2021: Evolution of the tropical response to periodic extratropical thermal forcing. J. Climate, 34, 6335–6353, https://doi.org/10.1175/JCLI-D-20-0493.1.
- Smith, D. M., and Coauthors, 2016: Role of volcanic and anthropogenic aerosols in the recent global surface warming slow-down. Nat. Climate Change, 6, 936–940, https://doi.org/10.1038/nclimate3058.
- Smith, T. M., R. W. Reynolds, T. C. Peterson, and J. Lawrimore, 2008: Improvements to NOAA's historical merged landocean surface temperature analysis (1880–2006). J. Climate, 21, 2283–2296, https://doi.org/10.1175/2007JCLI2100.1.
- Stuecker, M. F., and Coauthors, 2020: Strong remote control of future equatorial warming by off-equatorial forcing. Nat. Climate Change, 10, 124–129, https://doi.org/10.1038/s41558-019-0667-6.
- Takahashi, C., and M. Watanabe, 2016: Pacific trade winds accelerated by aerosol forcing over the past two decades. Nat. Cli-mate Change, 6, 768–772, https://doi.org/10.1038/nclimate2996. Tardif, R., and Coauthors, 2019: Last Millennium Reanalysis with an expanded proxy database and seasonal proxy modeling.

 Climate Past, 15, 1251–1273, https://doi.org/10.5194/cp-15-1251-2019.
- Thompson, D. W., and S. Solomon, 2002: Interpretation of recent Southern Hemisphere climate change. Science, 296, 895–899, https://doi.org/10.1126/science.1069270.
- Turner, J., T. J. Bracegirdle, T. Phillips, G. J. Marshall, and J. S. Hosking, 2013: An initial assessment of Antarctic sea ice extent in the CMIP5 models. J. Climate, 26, 1473–1484, https://doi.org/10.1175/JCLI-D-12-00068.1.
- Wang, C., 2006: An overlooked feature of tropical climate: Inter-Pacific-Atlantic variability. Geophys. Res. Lett., 33, L12702, https://doi.org/10.1029/2006GL026324.
- Watanabe, M., J. L. Dufresne, Y. Kosaka, T. Mauritsen, and H. Tatebe, 2021: Enhanced warming constrained by past trends in equatorial Pacific sea surface temperature

- gradient. Nat. Climate Change, 11, 33–37, https://doi.org/10.1038/s41558-020-00933-3.
- Wood, R., and C. S. Bretherton, 2006: On the relationship between stratiform low cloud cover and lower-tropospheric stability. J. Climate, 19, 6425–6432, https://doi.org/10.1175/JCLI3988.1.
- Xie, S.-P., and S. G. H. Philander, 1994: A coupled ocean-atmosphere model of relevance to the ITCZ in the eastern Pacific. Tellus, 46A, 340–350, https://doi.org/10.3402/tellusa.v46i4.15484.
- Yuan, X., M. R. Kaplan, and M. A. Cane, 2018: The interconnected global climate system}A review of tropical-polar teleconnections. J. Climate, 31, 5765–5792, https://doi.org/10.1175/JCLI-D-16-0637.1.
- Zhang, H., and Coauthors, 2018: East Asian hydroclimate modulated by the position of the westerlies during Termination I. Science, 362, 580–583, https://doi.org/10.1126/science.aat9393.
- Zhang, L., T. L. Delworth, W. Cooke, and X. Yang, 2019: Natural variability of Southern Ocean convection as a driver of observed climate trends. Nat. Climate Change, 9, 59–65, https://doi.org/10.1038/s41558-018-0350-3.
- Zhang, X., C. Deser, and L. Sun, 2021: Is there a tropical response to recent observed Southern Ocean cooling? Geophys. Res. Lett., 48, e2020GL091235, https://doi.org/10.1029/2020GL091235.
- Zhou, C., M. D. Zelinka, and S. A. Klein, 2016: Impact of decadal cloud variations on the Earth's energy budget. Nat. Geosci., 9, 871–874, https://doi.org/10.1038/ngeo2828.